Solid State Technology
Volume: 63 Issue: 3
Publication Year: 2020

Transformer-less Single-phase Inverter Based on SPWM Technique for Standalone PV Application

Adel M. Dakhil [1], Ahmed Raisan Hussein [2] and Ameer L. Saleh [3]
[1,2,3] Department of Electrical Engineering, University of Misan, Misan, Iraq
ameer-lateef@uomisan.edu.iq

***Abstract*—** In standalone photovoltaic (PV) inverter a total cost and harmonic content are most two problems that should be satisfied. In general, the main problems of square and modified sine wave inverters are a higher harmonic content and present the low frequency (LF) or higher frequency (HF) transformer in its configuration. For this reason, this paper presents a single-phase transformer-less inverter for standalone PV application. A robust unipolar Sinusoidal Pulse Width Modulation (SPWM) control technique is presented to control the inverter switches and obtained a sinusoidal output current and voltage. The proposed inverter is incorporated with the boost converter to provide a high DC voltage level and maximum power point tracking (MPPT) technique from the PV system. The low cost perturb and observe (P&O) MPPT technique is used. The performance of the proposed inverter is evaluated using Physical Security Information Management (PSIM) software. Also, the proposed inverter has been capable to generate pure sin wave of voltage and current during all conditions, when it runs in variations of weather conditions or the load variations. Finally, a well THD content in output current waveform is achieved at different solar irradiation.

Keywords- *Transformer-less Inverter; Sinusoidal Pulse Width Modulation (SPWM); Standalone Photovoltaic inverter.*

1. INTRODUCTION

Fossil fuels had been widely used in most of the industrial revolution; therefore, the combustion is required, which is caused the store energy liberation. Besides, this process causes a release of emissions into the atmosphere, and then it produces environmental pollution. For this reason, renewable energy is earning more visibility, while the power demand of the world is growing due to its clean and free. Moreover, the renewable energy harvested by photovoltaic (PV) systems is readily available in most applications. Mainly, the PV systems applications can be divided into two applications; grid-connected applications and standalone applications [2,3]. In grid-connected applications, the PV system is integrated into the utility grid to inject Alternating Current (AC) to the grid with the same phase and frequency of the utility grid voltage. Sold-state inverters are to be the qualifying technology for setting PV systems into the utility grid. Connection of the PV power generation systems into the grid plays a significant role in ensuring the electric power supply in an environmentally friendly way [4]. Besides, these inverters have been used in a standalone or hybrid system depending on the application and requirements of the PV system. The conventional PV inverter with the help of batteries can be operated in standalone mode. This inverter store the energy during the day and transferred it to the load during the night where the solar energy is absent [5-8]. This inverter is more expensive due to it required a charge controller for batteries, a power step-up

transformer, and more maintenance labor. On the other hand, the standalone inverter works without a battery for a local load is cheaper than that works with a battery. It is able to supply the surplus power that extracted from the PV system during the day to the local load for few kilowatts [9,10]. In recent years, a large number of inverter configurations that could be used of standalone PV inverters are proposed and reviewed [11-15]. Type of the control strategies, use of the step-up transformer, and different switching could be adopted with each one of those configurations. Present a step-up transformer in the configuration of the PV inverter may increase the total system cost. Some inverters have been designed with a high frequency (HF) or a low frequency (LF) transformer such as in [16-18] a single-phase inverter works with flyback converter is presented. The proposed inverter was operated with a HF transformer to raising the output voltage of the PV system into a high voltage level, which is converted to AC voltage using the DC/AC converter. This inverter is required more mathematical analysis to obtain the transformer parameters. Besides, the additional cost of the transformer is required and then the total system cost is increased. Therefore, the transformer-less inverter is a suitable choice for the standalone PV system due to having a low cost and high reliability with higher efficiency [19-21]. In this paper, a transformer-less inverter with Sinusoidal Pulse Width Modulation (SPWM) control for standalone PV application is offered. The proposed inverter is designed to works with a local load without using a battery. Thus, the charger controller and battery cost are avoided, and then the total cost is reduced. However, The PV panels are connected in series to form the PV system (PV arrays). Moreover, the PV system characteristics depend on weather conditions. Therefore, in some cases the PV system voltage is not sufficient to meet the load requirements so, a DC/DC converter was utilized. In this paper, a low cost of boost converter has been used to amplify the PV system voltage and implement the MPPT technique. The proposed inverter consists of a PV system, a boost converter, and a DC/AC converter of H-bridge type. The overall system circuits have been built using PSIM software. PSIM is a simulation solution for all power electronics and renewable energy applications due to it easily handles any power converter or motor drive simulation. The proposed inverter is tested with different weather conditions to achieve his performance. Thus, a pure sin wave of the current and voltage are obtained with lower THD content in their waveforms.

2. PHOTOVOLTAIC CELL CHARACTERISTICS

The PV cell physics model in practical form can be represented using the single-diode equivalent circuit as depicts in “Fig.1” [22, 23]. This model consists of the photo source current, one diode, a series, and shunt resistances. The main advantage of this model is a simple configuration. Furthermore, the output current the PV cell (I) can be expressed as follows [23, 24]:

$$I = I_{PH} - I_D - \left[\frac{I + I\,R_S}{R_{SH}}\right] \quad (1)$$

where I_{PH} is the photo source current, I_D is “the diode current”, R_S is “the cell series resistance” and R_{SH} is “the cell shunt resistance”. The diode current can be written as [24]:

$$I_D = I_{01}\left[xp\left(\frac{I + I\,R_S}{\alpha\,V_T}\right) - 1\right] \quad (2)$$

where I_{01} is the diode saturation current, α is “the diode ideality factor”, and V_T is “the thermal voltage” , which is written as :

$$V_T = \frac{kT}{q} \quad (3)$$

where T is the cell temperature in Kelvin, k is the Boltzmann's constant, and q is the electron's charge. The

photo source current depends on the solar irradiation G and the cell temperature as:

$$I_{PH}(G,T) = I_{PH,STC} \cdot \left(1 + K_I \cdot (T - T_{STC})\right) \cdot \frac{G}{G_{STC}} \quad (4)$$

where the subscript STC represents the Standard Test Conditions for weather conditions are irradiation G_{STC} equal to $1000\ W/m^2$, T_{STC} equal to 25 °C, and air mass equal to 1.5.

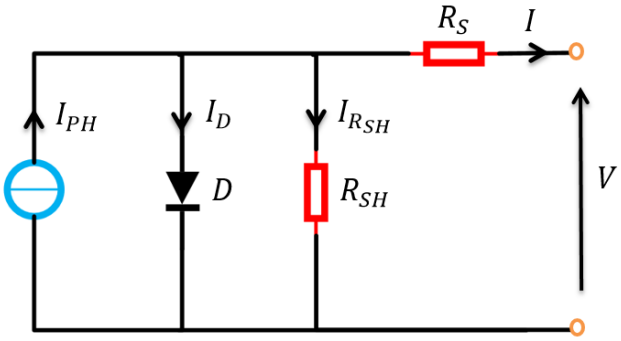

Figure 1. Equivalent circuit of the PV cell model.

Furthermore, the reverse saturation current of diode can be written as in Eq. (5), this current depends on the cell temperature as [22-24]:

$$I_0(T) = I_{0,STC}\left(\frac{T}{T_{STC}}\right) \cdot e^{\frac{E_g(T_{STC})}{\alpha \cdot k \cdot T_{STC}} - \frac{E_g(T)}{\alpha \cdot k \cdot T}} \quad (5)$$

where E_g is the energy of the bandgap of PN junction material. In general, its value equal to 1.12ev. However, the five parameters of the PV cell model at STC can be determined based on the electrical specification of the PV panel datasheet as presented in Table1. Thus, the five-parameter values are calculated in the methodology that cleared in [24].The PV panel that combined from many a series of cells can be provided a high output current and voltage. Also, based on the type of connection, these Panels are provided a high output current when it connected in parallel, and it provided a high output voltage in state of series connection. In this work, the nine PV panels of monocrystalline RICH-170W are connected in series to compose the proposed PV system with system requirements of 165V and 1500W voltage and power respectively.

Table 1 Electrical parameters of monocrystalline RICH SOLAR-170W datasheet.

Parameters	**Values**
$\boldsymbol{P_{MPP}}$	170W
$\boldsymbol{V_{MPP}}$	18.4V
$\boldsymbol{I_{MPP}}$	9.24A
$\boldsymbol{V_{OC}}$	22.6V
$\boldsymbol{I_{SC}}$	9.79A
Dimensions	58.7x26.8x1.4 in

The proposed PV system configuration is shown in "Fig.2", solar irradiation, G in W/m^2 and cell temperature T in ℃ represent the input values of the PV system. Besides, the terminals of the PV system are

connected to the boost converter to achieve the MPPT algorithm. Furthermore, the characteristics of the solar PV system are shown by P-V and I-V curve as presented in "Fig.3", for given solar irradiation and given fixed cell temperature. Moreover, the PV system can be operated with different operating points based on the resistive load value and environmental conditions. For this reason, an MPPT technique should be utilized to trace the maximum power point (MPP) from the PV system, which must be matched with the resistive load. In this paper, the perturbation and observation (P&O) MPPT technique is utilized. Due to its simplicity, easily, and lower cost. In this work, the PV system is designed to supply rated power with standard test conditions (STC) value of the solar irradiation as $G = 1000W/m^2$.

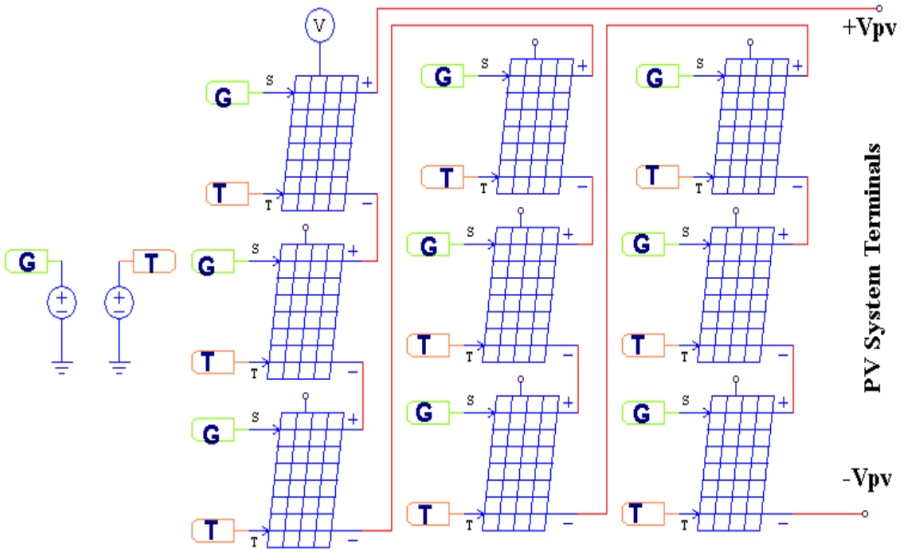

Figure 2. the proposed PV system configuration

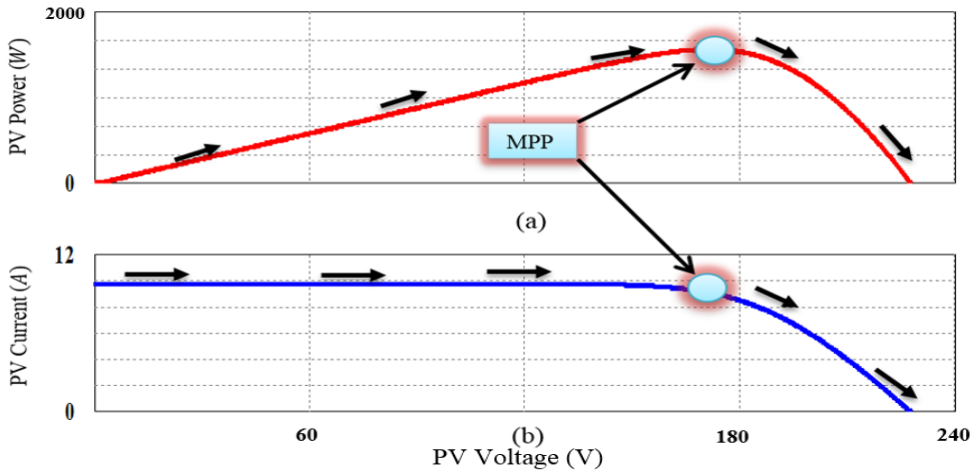

Figure 3. the PV system characteristics (a) P-V curve and (b) I-V curve.

3. PROPOSED SYSTEM DESIGN

3.1 Boost Converter with MPPT Technique

The block diagram of the proposed system is depicted in "Fig.4". The current and voltage of the PV system are sensed and then provided to the P&O algorithm to extract the MPP from the PV system for given irradiation and cell temperature. Hence, the duty cycle of the boost converter is controlled. The MOSFET switch of the boost converter is turned ON or OFF state based on the given PWM signal that produced by

comparison the duty cycle with the triangular carrier signal for the switching frequency about (20 kHz) as depicted in "Fig.5".

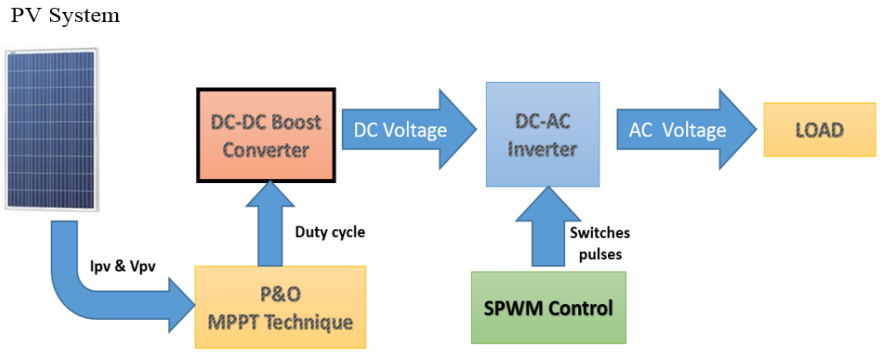

Figure 4. block diagram of the proposed system.

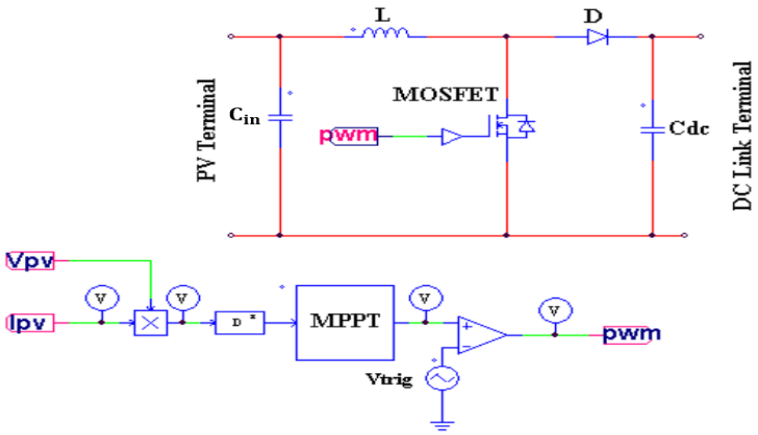

Figure 5. the proposed boost converter circuit with MPPT technique in PSIM software.

Furthermore, the boost converter can be operated with continuous condition (CCM) mode and discontinuous condition (DCM) mode depending on the inductor current shape [25,26]. In CCM mode, the inductor current flows continuously and does not reach zero as shown in "Fig.6". In this work, the boost converter is analyzed in CCM mode due to have the best performance and simple design. The boost circuit is adopted with CCM mode for ideal case (current through the switches at OFF state is zero and drop voltage across the switches at ON state is zero). When the MOSFET is in ON (closed), the input voltage V_{in} is applied across the inductor and causes a change in the inductor current (ΔL_{L-on}) as follows [25] :

$$\frac{\Delta L_{L-on}}{\Delta t} = \frac{V_{in}}{L} \tag{6}$$

At the interval end, the overall rise in inductor current can be expressed as:

$$\Delta L_{L-on} = \frac{1}{L}\int_0^{DT} V_{in}\, dt = \frac{DT}{L} V_{in} \tag{7}$$

where D is the duty ratio which represents the ratio of ON time of the MOSFET to the total switching time (T). At OFF time state, $V_L = V_{in} - V_{out}$, result:

$$V_{in} - V_{out} = L\, \frac{\Delta L_{L-off}}{\Delta_t} \tag{8}$$

The variation in (L_L) can be written as [26]:

$$\Delta L_{L-off} = \frac{1}{L}\int_0^{(1-D)T} \frac{V_{in} - V_{out}}{L}\, dt = \frac{V_{in} - V_{out}\,(1-D)T}{L} \quad (9)$$

In steady-state conditions for the boost converter, the inductor average voltage should be equal to zero during the total switching period, $T = T_{ON} + T_{OFF}$. So, the energy flows into the inductor over one switching cycle[25]. Therefore, L_L has the same value during the starting and the ending of the switching cycle, which can be written by:

$$\Delta L_{L-off} + \Delta L_{L-on} = 0 \quad (10)$$

$$\Delta L_{L-off} + \Delta L_{L-on} = \frac{V_{in}DT}{L} + \frac{V_{in} - V_{out}\,(1-D)T}{L} = 0 \quad (11)$$

Thus, the output voltage can be expressed as [26]:

$$V_{out} = \frac{V_{in}}{1-D} \quad (12)$$

And, the duty ratio can be explicated as:

$$D = 1 - \frac{V_{in}}{V_{out}} \quad (13)$$

Furthermore, from equation (13) the output voltage is always greater than the input voltage and it increases with an increase of duty cycle, D. Besides, the input voltage to the boost converter represents the output voltage of the PV system. Thus, the input voltage of the boost converter should be stepped-up to DC-link voltage level (400V). Therefore, the duty cycle value can be determined as,

$$D = 1 - \frac{V_{in}}{V_{out}} = 1 - \frac{165}{400} = 0.58$$

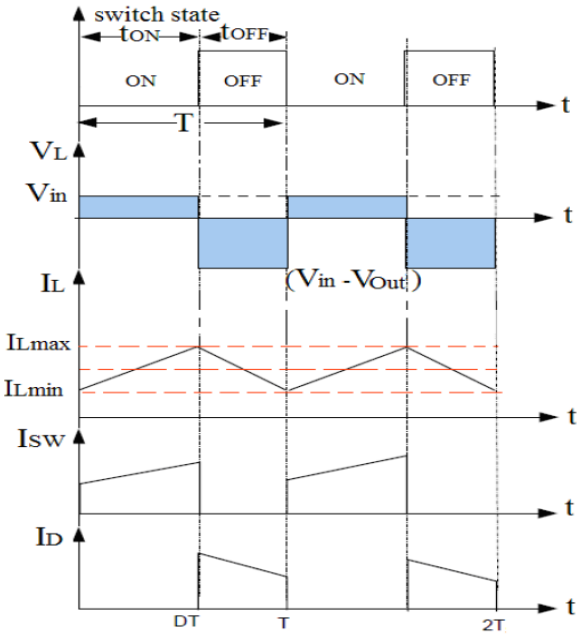

Figure 6. Key waveforms of boost converter at CCM [25].

From above, the equivalent input resistance R_{in}or the resistance that is seen by the PV system can be written as [25]:

$$R_{in} = \frac{R_L}{D^2} \quad (14)$$

where R_L is the load resistance. R_{in} depends on the duty cycle and load resistance, where the duty cycle D various from zero to 1, the input resistance various from infinity to R_L. The operating point of PV system characteristics is calculated by the intersection of the I-V curve with the load line with a slope of $I/V = 1/R_L$. Thus, by varying the duty cycle, the MPP is achieved when the load resistance in optimal value, and then the maximum power is delivered to the load.

3.2 Proposed Control Strategy

The output waveforms represent the main important aspect of an inverter topology. In general, the inverter topology can achieve two main different output AC waveforms as modified sine wave inverter and sine wave inverter [19]. The modified sine wave inverter is an upgrade to the square wave inverter, which is formed by three voltage levels in the output voltage $+V_{dc}$, - V_{dc}, and zero as presented in "Fig.7". This type of inverter is inexpensive as compared with the other inverters. The main problem of this inverter is harmonic content in its waveforms, thus, it used in some domestic electrical equipment. On the other hand, some appliances such as equipment's medical, variable speed devices, and printers may not work well in modified sin wave inverter. Therefore, the sin wave inverter should be used which is provide a pure sinusoidal AC waveform. In this inverter, the PWM technique is utilized to control the output voltage magnitude and frequency, therefore, such an inverter called PWM inverter. Furthermore, the pure sin wave inverter can be controlled with a robust SPWM technique. SPWM is widely used due to it having a constant amplitude pulses with various pulse widths. The bipolar and unipolar are common techniques of SPWM, which are different in harmonic content in their output waveforms. Moreover, in the bipolar version, the output voltage can be controlled with one reference signal only. Thus, the output voltage is various between $+V_{dc}$ to - V_{dc} and then, the H-bridge inverter switches (S1, S2, S3 and S4) are turned ON or OFF simultaneously in the diagonal opposite manner as presented in "Fig.8'. In this paper, the unipolar SPWM control technique is used as presented in "Fig.9". In this technique, the output voltage alternates from $+V_{dc}$ to zero in the positive half and various from -V_{dc} to zero in the negative half. For this reason, a second comparator is used to compares the carrier triangle signal with the reference signals ($+V_{ref}$ and -V_{ref}). Therefore, the diagonally switches are not turned simultaneously. The state switches and the corresponding output voltage are indicated in "Fig.10".

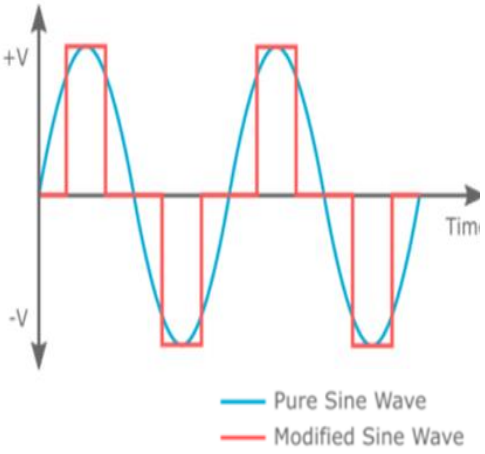

Figure 7. Modified and pure sin waves.

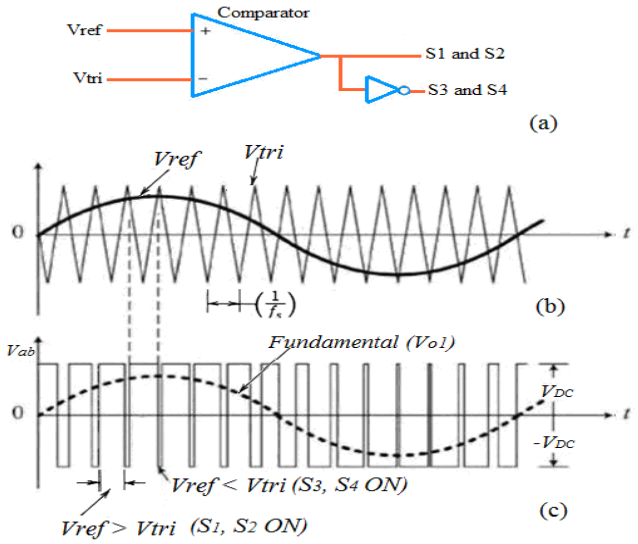

Figure 8. bipolar SPWM switching waveforms.

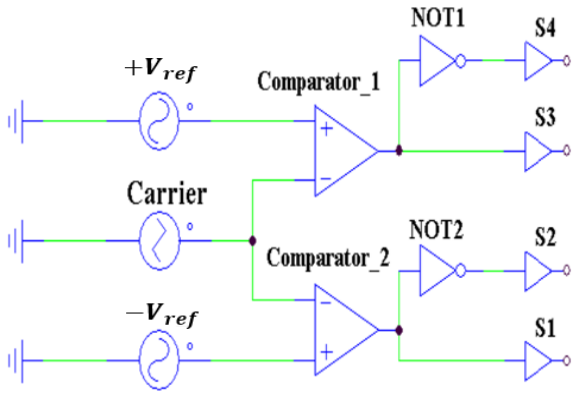

Figure 9. the proposed unipolar SPWM control technique.

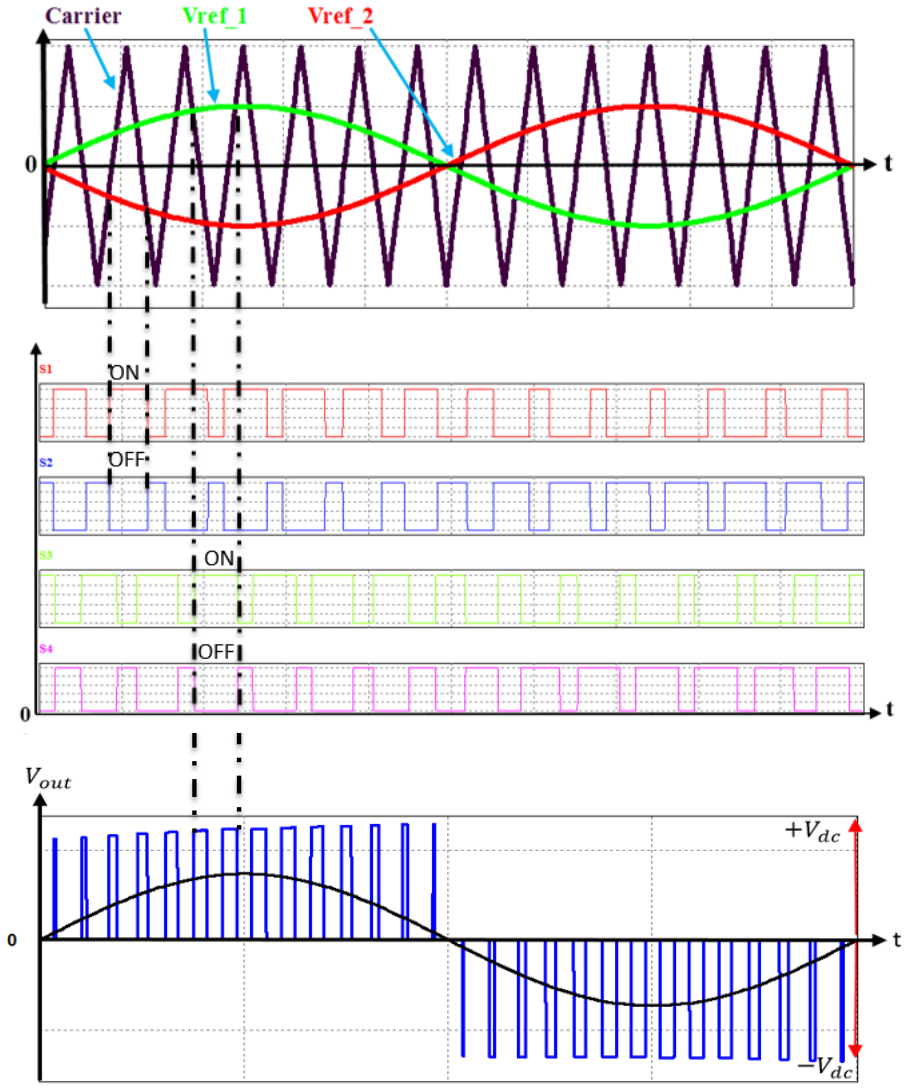

Figure 10. proposed state switches and the corresponding output voltage in unipolar SPWM technique.

In the proposed technique, the effective switching frequency is doubled. For this reason, the harmonic content of the output voltage and current is decreased compared with bipolar technique, this lead to reduce the filter size. However, the proposed model of the transformer-less inverter with the L-C filter is depicts in "Fig.11'. The DC-link capacitor is used between the boost converter and inverter to limit the output voltage ripple and support the load. Furthermore, the harmonic content in output current and voltage of the proposed inverter can be determined utilizing the total harmonic distortion (THD) equations as follows:

$$\%THD_v = \frac{\sqrt{\sum_{h=2}^{\infty} V_{h(RMS)}^2}}{V_{1(RMS)}} \times 100\% \quad (15)$$

$$\%THD_i = \frac{\sqrt{\sum_{h=2}^{\infty} I_{h(RMS)}^2}}{I_{1(RMS)}} \times 100\% \quad (16)$$

where $V_{h(RMS)}$ and $I_{h(RMS)}$ are the RMS values of h^{th} harmonic of the output voltage and current respectively. While $V_{1(RMS)}$ and $I_{1(RMS)}$ are the RMS values of fundamentals of the output voltage and current respectively. In this paper, the THD values of the voltage and current are calculated using Fast

Fourier Transfer (FFT) in PSIM software.

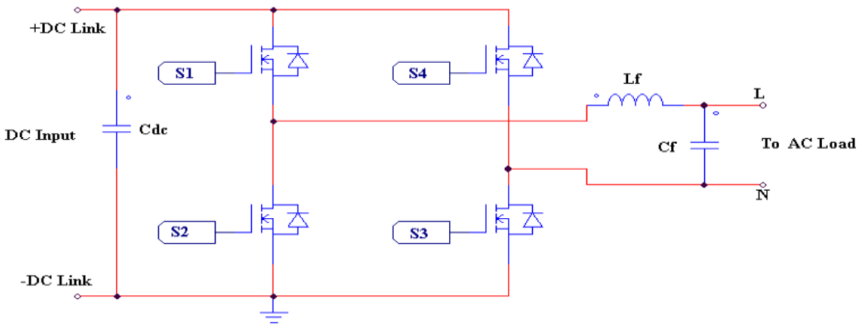

Figure 11. model of the transformer-less inverter with L-C filter in PSIM.

4. SIMULATION RESULTS AND DISCUSSION

The performance of the transformer-less inverter is evaluated using PSIM software. PSIM software is utilized to model and tested simulation of the overall circuits used in this work. The various operating conditions such as solar irradiation and cell temperature variation, and load changes take into account in simulation to test the performance and validity of the inverter. The simulation parameters of the proposed inverter are listed in table 2. The average values of current, voltage and power are 6A, 165V, and 1500W, respectively. A pure sin wave for output current and voltage are obtained in test performance of the proposed inverter as illustrated in "Fig.12". Besides, these results are taken for a resistive load $R = 25\Omega$ and constant weather conditions at STC . As presented in "Fig. 13", the amplitude of inverter voltage before filtering is alternated between the 400V and -400V after reaching o the steady-state conditions. The results shown a good performance of the SPWM technique during the constant weather condition and load. As can be seen, the small THD contents in both voltage and current are achieved ($THD_v = 3.3\%$ and $THD_i = 3\%$).

Table 2 The simulation parameters of the proposed inverter.

Parameters	Values
Maximum power of PV system P_{pv}	1500 W
Maximum output current $i_{o,RMS}$	7.2 A
output voltage $v_{o,RMS}$	230 V
Supply frequency f	50 Hz
Switching frequency f_s	20000 Hz
Total input capacitor C_{in}	10000μF
Boost inductor L	3 mH
DC link capacitor C_{dc}	4700μF
Filter capacitor C_f	4μF
Filter inductor L_f	8 mH

The proposed inverter has been tested with solar irradiation variations to shown the performance under weather conditions for the PV system as presented in 'Fig.13'. The inverter has been tested with a rapid

changing to half as $G = 1000W/m^2$ to $G = 500W/m^2$ at $time = 2sec$ and the resistive load is not changed which is set to $R = 25\Omega$. From this result, the PV power system is decreased from 1500W to 900W. While the output current is decreased from 7.2A to 6A, which means, the output current is approximately proportional to the solar irradiation. Therefore, a high output current is obtained in high irradiation.

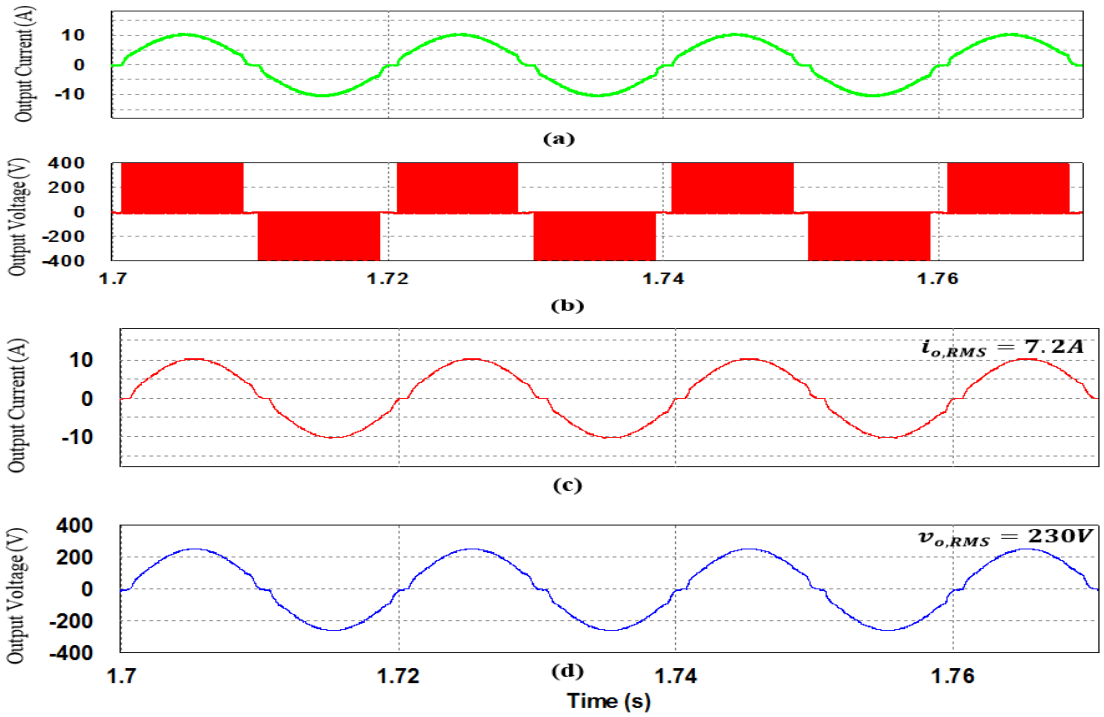

Figure 12. output current and voltage of the proposed inverter at $G = 1000W/m^2$ and $T = 25℃$ (a) output current before filtering (b) output voltage before filtering (c) output current after filtering (d) output voltage after filtering.

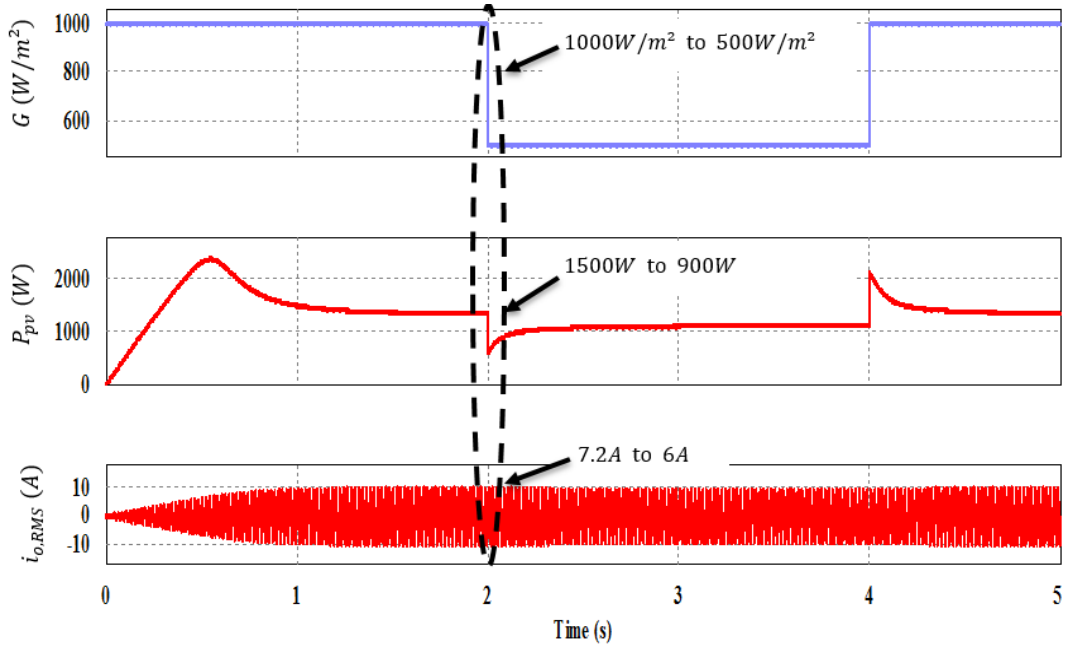

Figure 13. Simulation results of proposed inverter at the rapid changing of irradiation.

"Figure 14" depicts the output current waveform at step changing in the resistance of the load. Where the resistance is stepped up from $R = 25\Omega$ to $R = 50\Omega$, the output current is reduced from 7.2A to 4.8A. From this result, the output current value is effected strongly by changing the resistance of the load. Therefore, it decreased when the resistance of the load is increased but stay with its sinusoidal waveform as illustrated in "Fig.15".

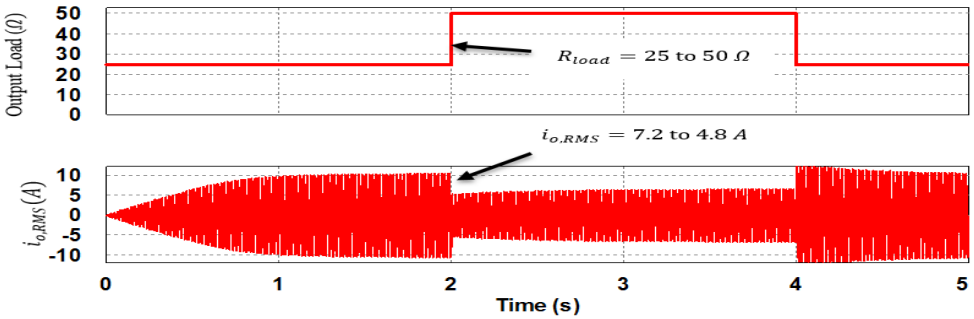

Figure 14. output current waveform with the step changing of the resistive load.

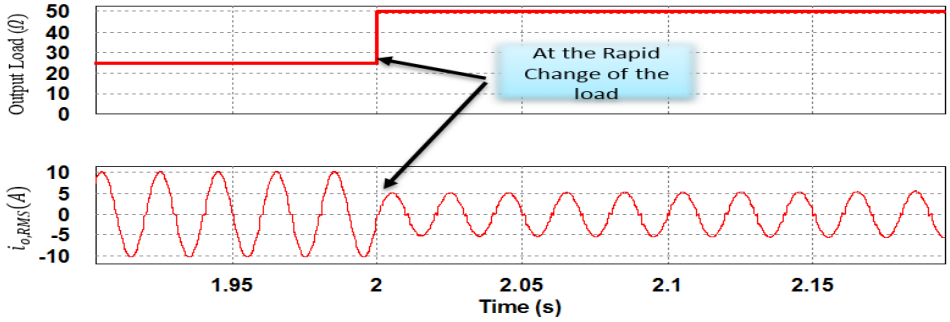

Figure 15. zoom of output current waveform with step changing of the resistive load.

From previous results, the proposed inverter gives the acceptable performance during all conditions when it runs in variations of weather conditions or the load variations. For this reason, the plot displays that the proposed inverter has been capable to generate pure sin wave of voltage and current at any conditions. Thus the aim of the proposed inverter is performed. Moreover, a well THD content in output current is achieved at different solar irradiation as presented in "Fig.16". High output current values are obtained in high irradiation, thus a well THD values are obtained. Besides, a poor value of THD is obtained during the lower irradiation.

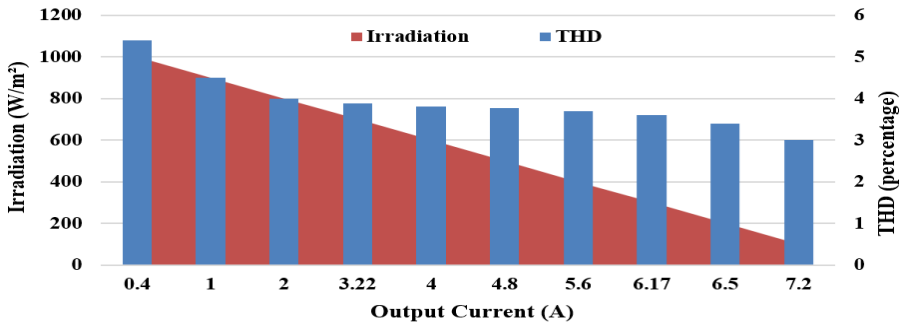

Figure 16. THD content in output current at different solar irradiation.

5. Conclusion

In this paper, a standalone transformer-less inverter is presented. Firstly, the solar PV cell

characteristics is analyzed mathematically based on the single-diode PV cell model. Secondly, the proposed inverter is connected to the boost converter and it is used to obtain the P&O-MPPT technique from the PV system. The boost circuit is designed with CCM mode due to its simplicity. The SPWM technique is used to control the inverter switches. The proposed control is tested with different weather and load conditions. Finally, pure sin wave waveforms for the output current and voltage are obtained with lower values of THD.

REFERENCES

[1] A. Khaligh and O. Oner, "Energy Harvesting Solar, Wind, and Ocean Energy Conversion Systems," Talyer and Franceis Group, ISBN: 978-1-4398-1508-3, U.S.A, 2010.

[2] M. Anwari,"Recent trends in renewable energy and power electronics research," Penerbit UTM University, Malaysia, ISBN 978-983-52-0639-9, 2008.

[3] C. L. Trujillo, F.Santamaria, and E. E. Gaona, "Modeling and Testing of Two- Stage Grid-connected Photovoltaic Micro-inverter," Elsevier publisher, Renewable Energy, Vol.99, pp.533-542, Jul.2016.

[4] Salam J. Yaqoob, A. A. Obed, "Photovoltaic Flybck Micro-inverter with Power Decoupling Technique," *Indonesian Journal of Electrical Engineering and Computer Science (IJEECS)*, Vol.15, No.1 pp. 9-19, Jul. 2019.

[5] K. Tamer, A. Ibrahim, and A. Mohamed, "A Review on Sizing Methodologies of Photovoltaic Array and Storage Battery in a Standalone Photovoltaic System," *Elsevier, Energy Conversion and Management*, Vol.120, pp.430-448, may, 2016.

[6] L. W. Chong, R. K Rajkumar, and D. Isa, "An optimal control strategy for standalone PV system with Battery-Supercapacitor Hybrid Energy Storage System," Elsevier, *Journal of Power Sources*, Vol.331, pp.553-565. Sep. 2016.

[7] L. Maheswari, P. S. Rao, N. Sivakumaran, G. S. Ilango, and C. Nagamani, "A Control Strategy to Enhance the Life Time of The Battery in a Stand-alone PV System with DC Loads," *IET Power Electronics*, Vol.10,No. 9, pp.1087-1094.Jun. 2017.

[8] L. W Chong, Y. W. Wong, R. K. Rajkumarand, and D. Isa, "An Adaptive Learning Control Strategy for Standalone PV System with Battery-supercapacitor Hybrid Energy Storage System," *Elsevier, Journal of Power Sources, 394*, 35-49. 2018.

[9] Cao, D., Jiang, S., Yu, X., & Peng, F. Z. (2011). "Low-cost semi-Z-source inverter for single-phase photovoltaic systems," *IEEE Transactions on Power electronics*, Vol.26, No.12, pp.3514-3523. Dec. 2011.

[10] Y. Shi, Z. Pan, R. Rodrigues and C. Wei, "A Low-cost Single-stage PV Inverter," *IEEE, Applied Power Electronics Conference and Exposition (APEC)*, pp. 387-392.Mar. 2018.

[11] Kumar, Nayan, Tapas Kumar Saha, and Jayati Dey, "Sliding mode Control, Implementation and Performance Analysis of Standalone PV Fed Dual Inverter," *Elsevier, Solar Energy*, Vol.155, pp.1178-1187.Jul. 2017.

[12] S. Kumar and Y. Pal, "A Three-Phase Asymmetric Multilevel Inverter for Standalone PV Systems," *IEEE, 6th International Conference on Signal Processing and Integrated Networks (SPIN)*, pp. 357-361, Mar. 2019.

[13] W. Ali, H. Farooq, A. U. Rehman, Q. Awais, M. Jamil, and A. Noman, "Design Considerations of Stand-alone Solar Photovoltaic Systems," IEEE, *International Conference on Computing, Electronic and Electrical Engineering (ICE Cube)*, pp. 1-6, Nov. 2018.

[14] Nordin, Nur Dalilah, and H. Abdul Rahman. "A Novel Optimization Method for Designing Standalone Photovoltaic System," *Elsevier*

Renewable Energy, Vol. 89, pp.706-715. 2016.

[15] Bhukya, Muralidhar Nayak, Venkata Reddy Kota, and Shobha Rani Depuru "A Simple, Efficient, and Novel Standalone Photovoltaic Inverter Configuration with Reduced Harmonic Distortion," *IEEE Access* 7 (2019): 43831-43845.

[16] C. L. Trujillo, F.Santamaria, and E. E. Gaona, "Modeling and Testing of Two- Stage Grid-connected Photovoltaic Micro-inverter," *Elsevier publisher, Renewable Energy*, Vol.99, pp.533-542, Jul.2016.

[17] Y. H. Kim, Y. H. Ji, J. G. Kim, Y. C. Jung, and C. Y. Won, "A New Control Strategy for Improving Weighted Efficiency in Photovoltaic AC Module-Type Interleaved Flyback Inverters," *IEEE Transactions on Power Electronics,* Vol. 28, No. 6, pp. 2688 - 2699, Jun. 2013

[18] J. Jan, Y. Kim, D. Ryu, C. Won, and Y. Jung, "High Efficiency Control Method for Interleaved Flyback Inverter with Synchronous Rectifier Based on Photovoltaic AC Modules," *IEEE, 38th Annual Conference in Industrial Electronics Society (IECON)*, pp.5720-5725, Oct. 2012.

[19] A. Chemseddine, N. Benabadji, A. Cheknane, and S. E. Mankour, "A comparison of single phase standalone square waveform solar inverter topologies: Half bridge and full bridge,"*International Journal of Electrical & Computer Engineering,* Vol. 10, No. 4, pp.3384-3392. Aug. 2020.

[20] P. J. Sudarshan, K. C. Swamy, P. Nagarajaand J. Manohar, "A Novel Transformer Less SPWM Inverter using DC-DC Boost Converter with Coupled Inductor for Standalone Applications," In *2016 International Conference on Computation of Power, Energy Information and Commuincation (ICCPEIC)*, pp. 581-586). Apr. 2016.

[21] P. Raseena, "Transformerless Photovoltaic Inverter for Standalone Scheme with Extended Input Voltage," *Materials Today: Proceedings, Vol. 24*, pp.1965-1971. 2020.

[22] A. N. Celik and N. Acikgoz, "Modeling and Experimental Verification of the Operating Current of Mono-crystalline Photovoltaic Modules Using Four and Five Parameter Models," *Elsevier publisher, Applied Energy,* Vol. 84, pp.1-15, Jun. 2007.

[23] M. G. Villalva, J. R. Gazoli, and E. R. Filho, "Comprehensive Approach to Modeling and Simulation of Photovoltaic Arrays," *IEEE Transactions on Power Electronics* Vol. 42, No. 5, May, 2009.

[24] S. J. Yaqoob, and Adel A. Obed, "Modeling, Simulation and Implementation of Photovoltaic Panel Model by Proteus Software Based on High Accuracy Two-diode Model," *Journal of Techniques* vol.1, no.1. pp.39-51, Dec. 2019.

[25] J. R. Mahmood , and N. H. Selman, "Control of the Output Voltage of the PV System Based DC-DC Boost Converter Using Arduino microcontroller," *International Journal of Science Engineering and Advance Technology*, Vol. 4, No.7, pp.322-331, Jul. 2016.

[26] Waleed I. Hameed, Ameer L. Saleh, Baha A. Sawadi , Yasir I. A. Al-Yasir and Raed A. Abd-Alhameed. "Maximum power point tracking for photovoltaic system by using fuzzy neural network," *Inventions,* Vol.4, No. 33,2019.